SCIENCE OF THE TOTAL ENVIRONMENT XX (2008) XXX–XXX

available at www.sciencedirect.com

ScienceDirect

www.elsevier.com/locate/scitotenv

A method for upscaling soil parameters for use in a dynamic modelling assessment of water quality in the Pyrenees

Lluís Camarero[a,*], *Jordi Garcia-Pausas*[b], *Carme Huguet*[c]

[a]*Centre d'Estudis Avançats de Blanes CEAB-CSIC, Accés Cala Sant Francesc 14, Blanes 17300, Girona, Spain*
[b]*Centre Tecnològic Forestal de Catalunya, Ctra. Vella de St. Llorenç km 2, 25280 Solsona, Spain*
[c]*School of Oceanography, Box 355351, University of Washington, Seattle, Washington 98195-5351, USA*

ARTICLE DATA

Article history:
Received 23 May 2008
Received in revised form
11 October 2008
Accepted 14 October 2008

Keywords:
Cation exchange capacity
Soil base saturation
Soil organic content
Lake water chemistry
Acidification recovery
Pyrenees

ABSTRACT

Dynamic modelling of hydrochemistry is a valuable tool to study and predict the recovery of surface waters from acidification, and to assess the effects of confounding factors (such as delayed soil response and changing climate) that cause hysteresis during reversal from acidification. The availability of soil data is often a limitation for the regional application of dynamic models. Here we present a method to upscale site-specific soil properties to a regional scale in order to circumvent that problem. The method proposed for upscaling relied on multiple regression models between soil properties and a suite of environmental variables used as predictors. Soil measurements were made during a field survey in 13 catchments in the Pyrenees (NW Spain). The environmental variables were derived from mapped or remotely sensed topographic, lithological, land-cover, and climatic information. Regression models were then used to model soil parameters, which were supplied as input for the biogeochemical model MAGIC (Model for Acidification of Groundwater In Catchments) in order to reconstruct the history of acidification in Pyrenean lakes and forecast the recovery under a scenario of reduced acid deposition. The resulting simulations were then compared with model runs using field measurements as input parameters. These comparisons showed that regional averages for the key water and soil chemistry variables were suitably reproduced when using the modelled parameters. Simulations of water chemistry at the catchment scale also showed good results, whereas simulated soil parameters reflected uncertainty in the initial modelled estimates.

1. Introduction

Since the 19th century Industrial Revolution, soils and surface waters have been acidified in areas of Europe and North America as a result of the emission and subsequent deposition of S and N oxides from fossil fuel combustion (Rodhe et al., 1995). After the implementation of internationally agreed protocols for the reduction of emissions (e.g. UNECE's Convention on Long-range Transboundary Air Pollution protocols, http://www.unece.org/env/lrtap/status/lrtap_s.htm), even though uncertainty remains about the future of emissions in developing countries, acidification is reverting and recovery of aquatic ecosystems from this process has started (Stoddard et al., 1999). However, there is hysteresis in the recovery process (Kopáček et al., 2002) which was initially explained by the delay caused by a 'buffering' effect of soils, owing to desorption of SO_4^{2-} from previously acidified soils (Prechtel et al., 2001). More recently, the effect of confounding climatic factors on recovery from acidification has been highlighted by Wright et al. (2006).

A useful approach to study recovery is through dynamic biogeochemical modelling applied on a regional scale (Hettelingh et al., 2003), not only in previously acidified areas, but also in regions where no severe acidification has occurred. In this regard, the Pyrenees, which show little acidification, are

* *Corresponding author*. Tel.: +34 972 336 101; fax: +34 972 337 806.
E-mail address: camarero@ceab.csic.es (L. Camarero).

0048-9697/$ – see front matter © 2008 Elsevier B.V. All rights reserved.
doi:10.1016/j.scitotenv.2008.10.035

a reference lake district in Europe and their study may help to disentangle climate- induced changes from acidification recovery. Most Pyrenean lakes lie on crystalline bedrocks with a composition comparable to that of the most acid-sensitive regions undergoing recovery in the northern hemisphere; however, they have received low deposition loadings and minimal acidification of soils and surface waters (Camarero and Catalan, 1998). The dynamic model MAGIC has already been applied in the Pyrenees as a single catchment application (Camarero et al., 2004; Wright et al., 2006) and as a regional application (Wright et al., 2005).

Soil physico-chemical properties are a crucial input for dynamic models, however, the lack of detailed soil information is often a shortcoming for regional applications, and results in a need to upscale the limited information available over the whole region of interest, as is the case for the Pyrenees. In general terms, upscaling involves taking a model that is applicable at a site-specific scale (at which observations are made), and projecting the outcome in a way that it is applicable at a larger scale (regional or global). One of the main problems encountered when upscaling occurs when single-site observations do not represent spatial heterogeneity of the parameters or variables at larger spatial scales (Harvey, 2000). Thus, knowledge of the specific spatial distribution of the model input parameters is required. Several techniques have been used to upscale the distribution of soil parameters. For instance, Helliwell et al. (1998) applied and compared two geostatistical methods to estimate soil parameters from point-source information in Scottish soil databases. Our main hypothesis was that it is possible to infer soil parameters from a set of environmental variables, which can be obtained from available mapped and remote sensed information, and that these inferred soil parameters are accurate enough to be used in dynamic modelling of lake water chemistry. To demonstrate this, we chose to model soil input parameters as a function of available environmental spatial information in the Pyrenees lake district. The kind of modelling used consists of simple parameterisations that represent the effects of unresolved processes without attempting to represent the processes themselves or the quantitative relationships that govern them; in other words, we addressed empirical cause–effect relationships.

The main aim of this study was to examine the empirical relationships between soil parameters relevant for dynamic modelling and various environmental parameters (topography, geographic location, lithology, vegetation, land-cover, and atmospheric deposition) using multiple regression techniques. We also tested the value of the estimates of soil parameters obtained from these regression models when used as inputs for the hydrochemical model MAGIC.

2. Material and methods

2.1. Study area

This study was carried out in an area characterised by subalpine and alpine soils along the Pyrenean range (NW Spain) (Fig. 1) during the summer of 2001. We visited 22 catchments, and a total number of 36 soil pits were sampled. The catchments selected were distributed along the whole mountain range within a wide range of altitudes (from 1845 to 2900 m asl), slopes and aspects, therefore including different climatic conditions and vegetation coverage. The sampling locations were selected in order to get a representative sample of the main lithologies in the Pyrenees. Granites and slates are the most extended lithologies in the Pyrenees, but in the central and western areas, granite peaks are flanked by layers of limestone, which are also abundant. Lake chemistry was used as the primary indicator of the underlying geology of the catchments. None of the catchments in this study is submitted to an intensive land use (forestry or agricultural activities) and most of them lie within wild, high mountain protected areas. Only in some cases, the lower part of the catchment is occasionally visited in summer by cattle or sheep in reduced numbers. Climatic conditions were typically alpine with cold mean annual temperatures that ranged between −0.7 and 5 °C, and high mean annual precipitation (between 1416 and 1904 mm) well distributed throughout the year. Soils are usually thin and, despite the presence of carbonated bedrocks in some areas, they consistently have a low pH due to the high rainfall.

2.2. Soil sampling, analysis and estimation of parameters

In the field, we identified and mapped the main 'soil units' at each catchment, i.e. areas that may be assumed to be covered by an homogeneous type of soil. The main criterion used to define the soil units was vegetation as indicator of the kind of underlying soil. Vegetation in the catchments sampled was divided into different kinds of alpine meadows, shrubs, and forest. The distribution of vegetation generally corresponded to the main characteristics of the terrain, like aspect, slope, and altitude. The percentage of soil coverage within each of the soil units was established by consensus of three observers. The number of soil units in a catchment was between 1 and 3, depending on the characteristics and size of the catchment. At least one soil pit was sampled within each soil unit, usually in the central part.

At each sampling point, a soil pit was dug until the bedrock was reached, and total soil depth was recorded. The main topographic variables (altitude, aspect and slope) were also recorded. Then, between one and four horizons were delimited on the basis of visual differences such as colour and consistence. Surface horizons were defined in the field as the layer with the highest root density. For each profile, a soil sample from each horizon was taken with a 7-cm diameter PVC corer, which was also used to determine soil bulk density. All samples were sieved in the field with a 1-cm mesh to retrieve stones, which were weighed with a dynamometer and discarded.

In the laboratory, the fresh soil samples were sieved to 2 mm to remove gravel and roots and the fine earth obtained was air dried to determine the fine earth content (FEC). The samples were then ground for chemical analyses. Soil pH was measured using both distilled water (pH_W) and 0.01 M $CaCl_2$ (pH_S) extractions, with a mass ratio of the air-dried fine earth to liquid phase of 1:5 after a 2.5-hour extraction with an orbital shaker. Exchangeable base cations ($BC_{ex} = Ca^{2+}_{ex} + Mg^{2+}_{ex} + Na^{+}_{ex} + K^{+}_{ex}$) and exchangeable acidity (Al^{3+}_{ex} and H^{+}_{ex}) were determined by extracting 1.25 g of air-dried fine earth with 25 ml of a 1 M NH_4Cl and a 1 M KCl solution, respectively. In the extracts, base cations were measured using the inductively

Please cite this article as: Camarero L, et al, A method for upscaling soil parameters for use in a dynamic modelling assessment of water quality in the Pyrenees, Sci Total Environ (2008), doi:10.1016/j.scitotenv.2008.10.035

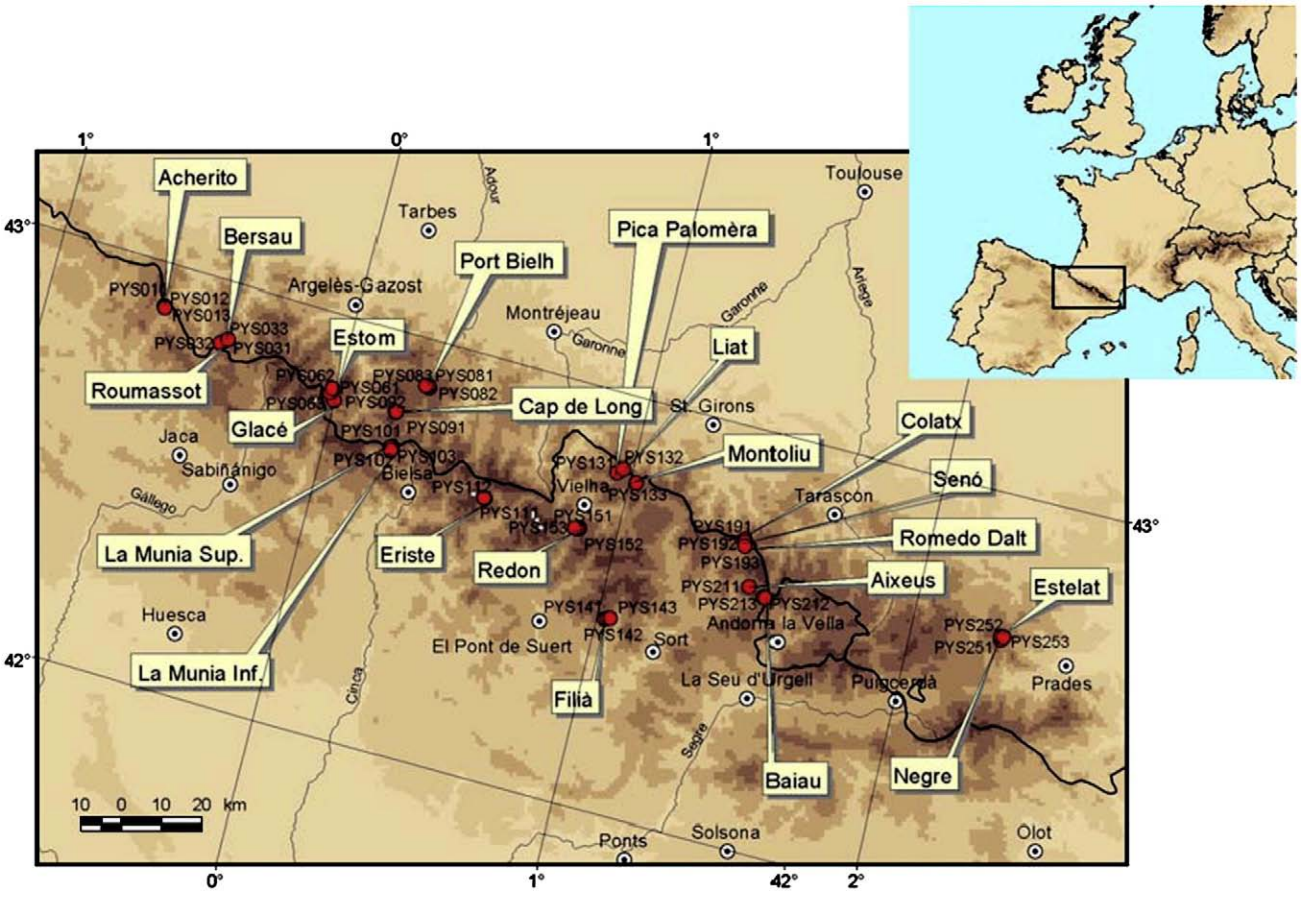

Fig. 1 – Map of the study area and location of the catchments (labels) and soil pits (circles) sampled.

coupled plasma technique (Thermo Jarrel Ash), and Al^{3+}_{ex} and H^{+}_{ex} were determined following Thomas (1982), by titration with 0.02 *N* NaOH to pH=8.2. Cation exchange capacity (CEC) was the sum of $BC_{ex}+Al^{3+}_{ex}+H^{+}_{ex}$, all concentrations being expressed as meq kg^{-1}. Base saturation (BS) was given as the percentage of BC_{ex} in CEC. Organic carbon (OC) and nitrogen (ON) were measured using an EA 1108 CHNS-O Carlo Erba analyser. All the samples were free of carbonates. Presence of carbonates was tested in the field by adding HCl to the fresh soil sample and observing effervescence.

A single lumped value for each physico-chemical soil parameter was estimated for each lake catchment. The use of catchment-lumped parameters is justified by the structure of MAGIC, the dynamic model chosen for this study (see Section 2.4). Detailed mechanistic models including explicitly the within-catchment heterogeneity would be very difficult (or even impossible) to upscale, and the trade between the loss of fine grain information and gain in spatial extension is inevitable.

To obtain the lumped soil parameters, a single value was first obtained for each pit by averaging the measurements from each sampled horizon, weighted by the amount of soil (fine earth) of each horizon as follows:

$$X_p = \sum_{1,h}\left(X_h \times FEC_h \times depth_h\right) / \sum_{1,h}\left(FEC_h \times depth_h\right) \quad (1)$$

where X_p is the averaged parameter for each pit, FEC_h is the FEC for a single horizon in kg m^{-3}, and $depth_h$ is the horizon depth in m. The total amount of soil (TAS, in kg) in the catchment was calculated as:

$$TAS = \sum_{1,p}\left(FEC_p \times depth_p \times A_p\right) \quad (2)$$

where $depth_p$ is the total depth (m) of each pit, and A_p (m^2) is the area of the soil unit of which each pit was considered to be representative within the catchment, and FEC_p is the volume weighted FEC of each pit calculated as:

$$FEC_p = \sum_{1,h}\left(FEC_h \times depth_h\right) / \sum_{1,h} depth_h \quad (3)$$

The lumped pooled catchment parameters where then computed as:

$$X_L = \sum_{1,p}\left(X_p \times FEC_p \times depth_p \times A_p\right) / TAS \quad (4)$$

The lumped base saturation (BS) was computed from the lumped amount of exchangeable bases and CEC.

Catchment soil depth ($depth_c$) was computed as the average depth weighted by the coverage of each soil unit, including areas without soil:

$$depth_c = \sum_{1,p}\left(depth_p \times A_p\right) / A_c \quad (5)$$

where A_c is the catchment area.

Please cite this article as: Camarero L, et al, A method for upscaling soil parameters for use in a dynamic modelling assessment of water quality in the Pyrenees, Sci Total Environ (2008), doi:10.1016/j.scitotenv.2008.10.035

Table 1 – Rock classes and the weight assigned to each class to compute the lithological parameter (LP)

Class	Code	Weight	Rocks
Detritic acid rocks	DetA	1	Carboniferous sandstones, lutites and black conglomerates
Plutonic, low soluble rocks	PluA	2	Bassiers monzogranite, tonalites, Néouvielle granodiorite
Metamorphic acidic rocks	MetA	3	Silurian slates
Detritic basic rocks	DetB	4	Quartz conglomerates and Cambrian–Ordovician sandstones
Plutonic, soluble rocks	PluB	5	Maladeta and Mont Louis granodiorites
Metamorphic basic rocks	MetB	6	Devonian and Cambrian–Ordovician shales
Carbonated rocks	Carb	7	Limestones
Detritic ultra-basic rocks	DetUB	8	Sandy pelites and carbonates

C pools in the whole catchment (C_{pool}, in kg m^{-2}) were calculated as:

$$C_{pool} = \sum_{1,p}\left(OC_p \times FEC_p \times depth_p \times A_p\right)/A_c \quad (6)$$

where OC_p is the OC concentration averaged for each pit. *N* pools were calculated similarly.

These lumped parameters were used to construct models to predict the soil properties to be used as input parameters for dynamic modelling. The models were estimated by stepwise multiple regression analysis using the S-PLUS 2000 software package (Insightful Corp.). For each soil parameter to be predicted, all the environmental variables to be tested are massively introduced in the stepwise analysis as potential predictors. The algorithm then selects only those predictors that contribute to explain significantly a part of the variability of the soil parameter data set, and constructs the multiple regression model using these selected predictors.

2.3. *Environmental variables*

The environmental variables used in our analyses included geographic, lithological, landcover, and climatic parameters.

Table 2 – Main descriptors of the catchments and lakes included in this study

	Catchment									Lake					
	Latitude	Longitude	Lowest altitude	Highest altitude	Area	Steepness index	Aspect	PPT	LP	Area	RT_W	Alk_G	ΣBC	SO_4^{2-}	NO_3^-
			m asl	m asl	km^2			m yr^{-1}		ha	months	μeq l^{-1}	μeq l^{-1}	μeq l^{-1}	μeq l^{-1}
Acherito	42°52'51" N	00°42'22" W	1875	2147	0.57	0.478	SW	1.544	2.2	5.7	7.7	957	996	41	4
Bersau	42°50'26" N	00°29'40" W	2077	2384	0.61	0.500	N	1.597	4.0	12.3	31.2	208	253	16	0
Roumassot	42°50'57" N	00°28'41" W	1845	2384	2.68	0.201	NE	1.485	5.2	5.0	1.2	383	364	21	0
Estom	42°48'27" N	00°05'55" W	1804	2976	11.45	0.102	N	1.416	3.8	6.2	0.5	345	383	40	10
Glacé	42°46'42" N	00°05'18" W	2571	2924	0.78	0.455	NE	1.779	6.2	6.2	8.6	380	432	42	14
Gourg Cap de Long	42°47'42" N	00°06'47" E	2845	3173	0.47	0.701	N	1.904	8.0	1.6	0.3	387	804	460	3
La Munia Superior	42°42'22" N	00°07'30" E	2537	3005	1.09	0.429	SW	1.727	6.4	2.3	0.6	416	561	49	8
La Munia Inferior	42°42'09" N	00°07'34" E	2525	3005	1.63	0.294	SW	1.727	6.7	5.4	5.5	n.a.	n.a.	n.a.	n.a.
Port Bielh	42°52'27" N	00°11'18" E	2290	2724	1.72	0.252	SW	1.650	2.0	15.6	5.4	220	286	19	6
Eriste	42°38'47" N	00°28'05" E	2411	3369	5.40	0.177	S	1.638	5.1	3.8	0.6	138	196	24	10
Redó	42°38'31" N	00°46'46" E	2235	2632	1.53	0.260	S	1.543	5.0	24.1	47.5	45	86	26	11
Pica Palomèra	42°47'38" N	00°52'08" E	2308	2460	0.69	0.221	E	1.603	3.0	4.9	3.0	−26	142	181	3
Liat	42°48'24" N	00°52'26" E	2140	2714	1.77	0.325	NW	1.523	6.0	27.1	19.8	92	162	43	0
Montoliu	42°47'05" N	00°55'34" E	2375	2734	1.23	0.293	S	1.631	4.3	11.2	6.1	248	376	113	0
Filià	42°27'04" N	00°57'12" E	2140	2615	1.48	0.322	N	1.452	6.4	1.4	0.2	1330	1411	71	2
Senó	42°42'43" N	01°19'22" E	2130	2527	2.01	0.198	S	1.494	2.8	5.9	1.5	13	44	15	1
Romedo Dalt	42°42'22" N	01°19'29" E	2110	2527	2.60	0.161	S	1.483	2.4	11.9	7.6	14	39	16	2
Colatx	42°43'03" N	01°19'30" E	2217	2527	0.66	0.470	S	1.494	2.0	2.2	1.4	n.a.	n.a.	n.a.	n.a.
Aixeus	42°36'40" N	01°22'18" E	2370	2905	0.82	0.650	N	1.593	6.0	3.4	2.6	−13	378	407	18
Baiau	42°35'47" N	01°25'55" E	2480	2894	1.12	0.371	SW	1.648	6.0	7.9	6.3	−40	1038	1240	16
Negre	42°38'09" N	02°12'41" E	2083	2352	0.80	0.337	SE	1.565	4.7	4.5	4.8	160	194	29	1
Estelat	42°38'47" N	02°12'49" E	2021	2400	1.50	0.253	E	1.536	3.5	4.6	0.5	180	196	26	1

Latitude, longitude and lowest altitude correspond to the catchment (lake) outlet. n.a.: data not available. PPT: precipitation. LP: lithological parameter. RT_W: water renewal time. Alk_G: Gran alkalinity. ΣBC: sum of base cations.

Please cite this article as: Camarero L, et al, A method for upscaling soil parameters for use in a dynamic modelling assessment of water quality in the Pyrenees, Sci Total Environ (2008), doi:10.1016/j.scitotenv.2008.10.035

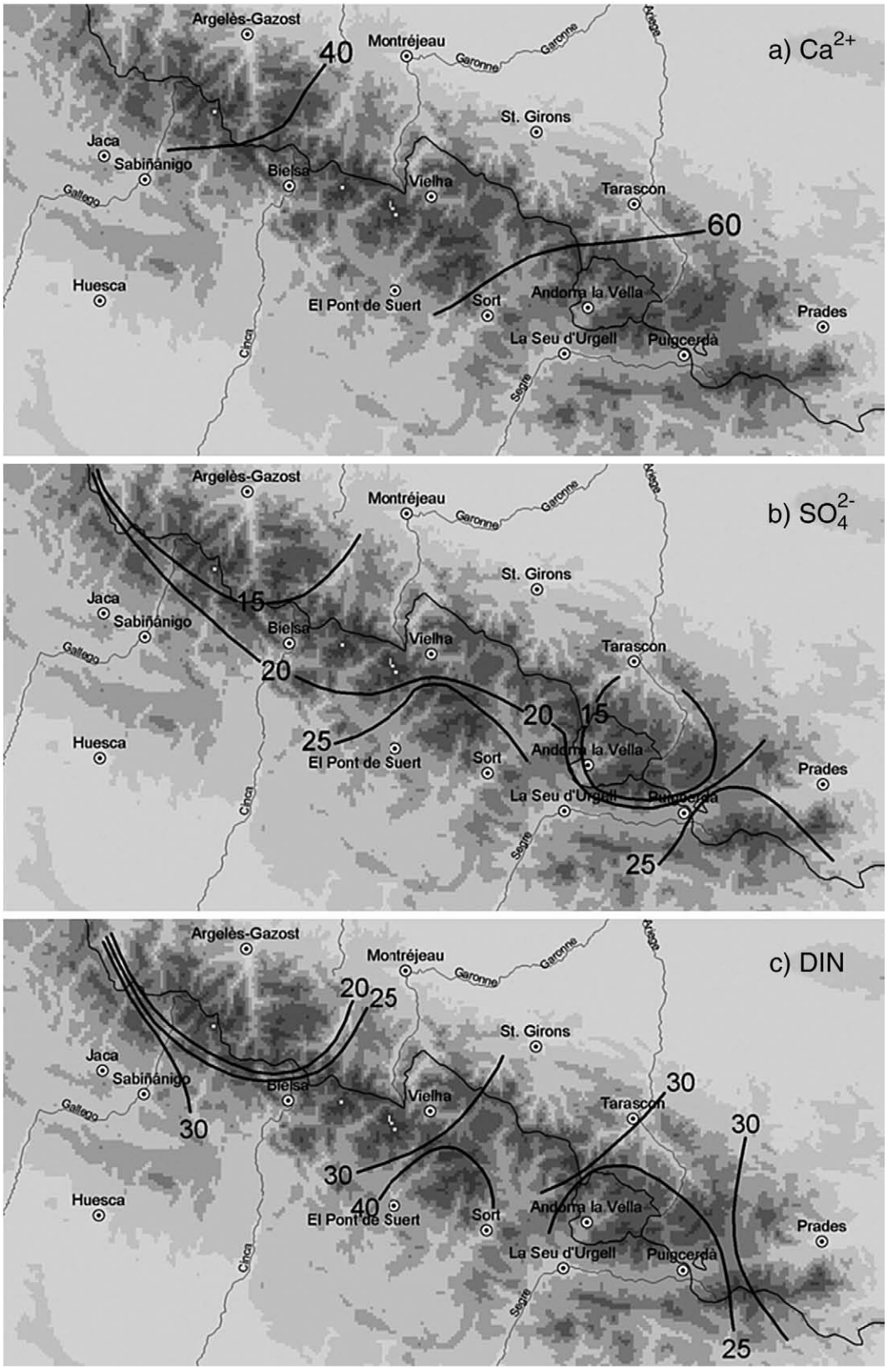

Fig. 2 – Geographic differences in the concentration of a) Ca^{2+}, b) SO_4^{2-} and c) $NO_3^- + NH_4^+$ (DIN: dissolved inorganic nitrogen) in atmospheric precipitation over the Pyrenees. Units are μeq l^{-1}.

Please cite this article as: Camarero L, et al, A method for upscaling soil parameters for use in a dynamic modelling assessment of water quality in the Pyrenees, Sci Total Environ (2008), doi:10.1016/j.scitotenv.2008.10.035

The geographic parameters were latitude, longitude, lowest and highest altitude, catchment aspect and area, and lake area and volume. They were obtained from maps and digital elevation models, using manual and computer-assisted GIS methods (ArcView GIS 3.2, Environmental Systems Research Institute Inc.). The aspect values (in degrees) referred to the main orientation of the catchment and were cosine-transformed to obtain a continuous variable that ranged between −1 (south) and 1 (north), with the same value (0) for the east and west aspects. Lake volume was estimated from lake area and maximum depth was estimated using an empirical hypsographic relationship for Pyrenean lakes provided by Catalan (pers. comm.). Additionally, the difference between lowest and highest altitude and the ratio of this difference and the catchment area (as an indicator of the steepness) were calculated and included in the multiple regression analysis.

The lithological composition of the catchments was extracted from 1:25 000 maps. The rocks observed were classified into 8 main groups and ranked on the basis of ease of weathering, i.e. their capacity to supply cations (Table 1). A weight was assigned to each rank and a lithological parameter (LP) was then computed for each catchment as the average of these weight values weighted by the proportion of each kind of rock in the catchment.

The landcover of the catchments was described as the percentage of area covered by glaciers, glacial deposits (moraines, screes, and boulders), bare rock, moorlands, peatlands, alpine meadows, shrubs, and coniferous woodlands. Most of this information was obtained from field observations, sometimes supported by vegetation maps and aerial photographs when available. The landcover information was used to calibrate a method to obtain the estimations of the percentage of soil coverage (SC) from satellite images (Casals-Carrasco et al., 2004), which was used as an input parameter in this study.

The mean monthly temperatures and precipitation values were obtained from a 30-year climate data series reconstructed following the method described by Agustí-Panareda and Thompson (2002). Estimates were obtained by stepwise multiple regression, which established linear functions between some existing upland records and many long lowland records. The mean annual temperature (*T*) and precipitation (PPT) data were derived from these estimations.

2.4. *MAGIC modelling*

MAGIC is a lumped-parameter model of intermediate complexity (Cosby et al., 1985a,b, 2001), and uses a lumped approach in two ways: 1) a myriad of chemical and biological processes active in catchments are aggregated into a few readily described processes; and 2) the spatial heterogeneity of soil properties within the catchment is lumped into one set of soil parameters. The model simulates soil solution and surface water chemistry to predict average concentrations of the major ions. Under the assumption of simultaneous reactions involving sulphate adsorption, cation exchange, dissolution–precipitation–speciation of aluminium and dissolution–speciation of inorganic and organic carbon, MAGIC simulates the concentrations of major ions on an annual time step. Nitrogen dynamics is modelled by simulating N saturation and links net immobilisation of N to the C/N ratio of the soil organic matter pool. MAGIC accounts for the mass balance of major ions in the soil by tracking the fluxes from atmospheric inputs, chemical weathering, net uptake in biomass and loss to runoff. Data inputs required for the calibration of MAGIC include lake and catchment characteristics, the chemical and physical characteristics of soil, input and output fluxes for water and major ions, net uptake of base cations and N by vegetation, and the supply of S by weathering.

The first step in MAGIC application is calibration. Calibration means that some parameters of the model, which are not directly measurable, have to be estimated. Some measured input parameters may also be adjusted, within a narrow tolerance margin, in order to improve the performance of the model. This calibration is done by finding the right values of the calibrated parameters which result in an output of the model that matches the observed target variables during the calibration period, in this case the actual chemistry of lakes.

MAGIC was calibrated in 20 of the lakes included in this study. Water chemistry was not available for the remaining two lakes. Lake water chemistry was obtained from a previous survey, in which lakes were sampled in July 2000 (Camarero et al., in press). This single measure is assumed to be representative of the average major ion chemistry of each lake. Some seasonal fluctuation may occur, but it should be much lower than the variability between lakes. All lakes share the general features of high mountain lakes. Water enters the lakes in a rather diffuse way, and when visible streams are present, they are markedly intermittent. All lakes have a single outlet. The outflow may stop in summer. The water level fluctuates by less than 1 m during the year. Water renewal time was estimated from lake volume, catchment area and precipitation, and differs between lakes (Table 2). Catchments generally had a rather impermeable bedrock; thin soils and

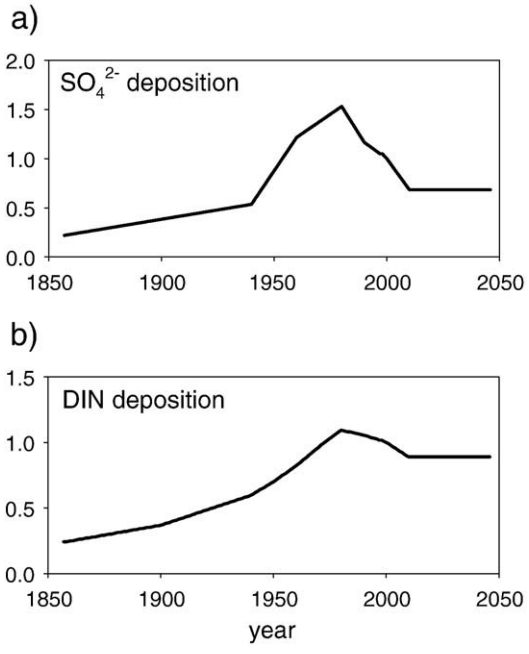

Fig. 3 – Deposition scenarios for a) SO_4^{2-} and b) DIN used in this study. Variations in deposition with time are expressed as a fraction of the year 2000 deposition.

Please cite this article as: Camarero L, et al, A method for upscaling soil parameters for use in a dynamic modelling assessment of water quality in the Pyrenees, Sci Total Environ (2008), doi:10.1016/j.scitotenv.2008.10.035

steep slopes contribute also to a quick flushing. Groundwater losses were therefore considered minor, and have been neglected in this study. Snow cover lasts from November–December until May–June, although some snowbeds may last longer at the highest areas in shaded zones. About half of the precipitation is in form of snow. Two calibrations were completed for comparison purposes, one using field measurements of soil parameters, and a second one using a set of parameters predicted with the multiple regression models using environmental variables. Gran alkalinity (Alk_G), the sum of base

Table 3 – Location and main characteristics of the soil pits sampled, with indication of the corresponding catchments

Name	Pit code	Latitude	Longitude	Altitude	Soil unit relative size[b]	Soil coverage[c]	Depth	FEC	pHs	CEC	BS	OC	C_{pool}	N_{pool}	CN
Lake/ catchment				m asl.	%	%	cm	kg m^{-3}		meq kg^{-1}	%	mol kg^{-1}	mol m^{-2}	mol m^{-2}	
Acherito	PYS011	42°53'09.2''N	00°42'25.6''W	1980	30	95	26	814	3.71	142	7.0	5.2	1094	92	11.9
	PYS012	42°52'60.0''N	00°42'19.6''W	1900	30	95	25	738	3.79	118	5.6	4.7	860	70	12.3
	PYS013	42°52'51.7''N	00°42'08.7''W	1910	10	20	24	875	3.81	121	6.6	4.0	846	74	11.4
Bersau	PYS031	42°50'25.4''N	00°29'30.7''W	2090	20	65	36	835	4.00	49	5.3	2.1	618	53	11.7
(23%)[a]	PYS032	42°50'13.8''N	00°29'52.3''W	2200	70	65	33	914	4.13	47	16.9	2.3	701	58	12.0
Roumassot	PYS033	42°51'03.8''N	00°28'39.5''W	1845	90	95	32	622	4.40	56	30.2	6.9	1355	87	15.7
(77%)															
Glacé (7%)[a]	PYS061	42°46'50.4''N	00°05'24.0''W	2750	40	10	13	367	4.01	111	26.9	8.1	386	26	14.7
Estom	PYS062	42°47'45.7''N	00°06'34.3''W	2200	45	17	26	248	4.02	102	17.1	5.8	371	25	15.1
(93%)	PYS063	42°48'26.0''N	00°06'11.8''W	1900	30	85	34	395	4.27	80	33.8	9.3	1247	79	15.7
Port Bielh	PYS081	42°52'15.6''N	00°11'58.4''E	2390	15	85	41	521	3.91	73	11.3	3.2	679	51	13.4
	PYS082	42°52'33.5''N	00°11'36.7''E	2340	15	85	28	570	3.98	74	9.3	5.8	933	67	14.0
	PYS083	42°52'25.6''N	00°11'08.9''E	2290	15	85	30	564	4.24	73	19.3	5.1	856	47	18.2
Gourg Cap de Long	PYS091	42°47'34.6''N	00°06'37.2''E	2900	5	10	38	385	4.76	75	83.5	4.1	604	44	13.7
La Munia	PYS101	42°42'34.0''N	00°07'39.3''E	2650	45	5	47	472	4.17	47	31.1	3.3	737	57	12.9
Superior	PYS102	42°42'27.8''N	00°07'22.3''E	2560	55	10	78	713	4.80	24	85.9	0.7	392	42	9.4
(67%)[a]															
La Munia Inferior (33%)	PYS103	42°42'04.4''N	00°07'33.0''E	2470	15	80	20	490	4.55	73	80.1	3.6	352	24	14.4
Eriste	PYS111	42°39'02.7''N	00°27'48.0''E	2450	1	100	35	485	4.14	72	22.3	7.2	1228	82	15.0
	PYS112	42°39'08.2''N	00°27'34.5''E	2470	30	10	27	714	4.04	84	21.2	7.3	1407	93	15.2
Pica Palomèra	PYS131	42°47'46.1''N	00°51'49.4''E	2380	100	70	30	883	3.88	36	14.1	4.3	1134	48	23.8
Liat	PYS132	42°48'29.6''N	00°52'47.6''E	2163	100	70	23	564	3.89	81	17.3	4.8	621	37	16.9
Montoliu	PYS133	42°47'02.4''N	00°55'55.4''E	2484	100	60	44	779	4.44	17	39.8	2.1	726	66	11.0
Filià	PYS141	42°26'47.1''N	00°56'16.4''E	2520	15	60	47	572	4.40	76	61.4	2.3	606	54	11.2
	PYS142	42°26'57.8''N	00°56'45.0''E	2260	40	95	53	613	4.27	38	27.0	1.7	560	51	11.0
	PYS143	42°27'05.3''N	00°57'16.0''E	2150	5	95	61	736	4.23	36	12.4	2.1	925	87	10.6
Redó	PYS151	42°38'34.0''N	00°47'10.1''E	2330	20	40	27	576	4.18	74	34.9	7.2	1116	71	15.8
	PYS152	42°38'25.5''N	00°46'54.9''E	2260	45	75	18	275	4.57	77	67.2	11.7	576	40	14.6
	PYS153	42°38'23.1''N	00°46'19.0''E	2370	35	75	32	526	4.16	66	24.1	6.3	1059	66	16.0
Colatx (25%)[a]	PYS191	42°43'14.2''N	01°19'17.3''E	2280	80	50	50	929	4.26	38	8.5	4.9	2283	164	13.9
Senó (52%)[a]	PYS192	42°42'54.5''N	01°19'21.0''E	2140	85	50	25	929	4.24	46	9.4	5.2	1202	82	14.6
Romedo Dalt (23%)	PYS193	42°42'15.5''N	01°19'33.3''E	2120	30	70	67	509	4.02	67	8.7	4.7	1618	103	15.7
Baiau	PYS211	42°35'45.5''N	01°25'29.2''E	2585	10	80	25	328	4.09	84	52.3	6.4	523	41	12.8
	PYS212	42°35'46.1''N	01°25'47.9''E	2490	15	80	76	730	4.68	16	64.6	1.0	551	56	9.8
Aixeus	PYS213	42°36'45.8''N	01°22'19.2''E	2470	25	70	24	594	4.00	71	30.6	7.2	999	65	15.4
Negre	PYS251	42°38'18.7''N	02°12'29.4''E	2140	100	85	20	612	4.49	98	72.6	4.0	492	31	15.7
Estelat	PYS252	42°38'48.4''N	02°12'15.9''E	2230	80	85	74	685	4.31	36	15.6	3.1	1558	111	14.1
	PYS253	42°38'47.5''N	02°12'52.6''E	1970	20	50	44	291	4.21	83	27.6	6.3	802	40	20.0

[a] Nested catchments: Bersau is a subcatchment of Roumassot; La Munia Superior is a subcatchment of La Munia Inferior; Glacé is a subcatchment of Estom; Colatx is a subcatchment of Senó, which is in turn a subcatchment of Romedo de Dalt. Percentages between brackets are the fraction of the total catchment area that contributes directly to the lake (direct catchment).

[b] Soil unit relative size: percentage of the direct catchment covered by the soil unit associated to each profile.

[c] Soil coverage: percentage of the soil unit covered by soil.

Please cite this article as: Camarero L, et al, A method for upscaling soil parameters for use in a dynamic modelling assessment of water quality in the Pyrenees, Sci Total Environ (2008), doi:10.1016/j.scitotenv.2008.10.035

cations (SBC), SO_4^{2-}, and NO_3^- concentrations in lake water are summarized in Table 2. Owing to the limited number of field measurements of atmospheric precipitation chemistry in the Pyrenees available, deposition patterns were extrapolated from previous measurements made at seven deposition collectors located within the region (Camarero and Catalan, 1993, 1996), EMEP S and N deposition models (Olendrzynski et al., 2000), and the deposition measured in 2000 in the Lake Redon station (42°38'36" N, 0°46'48" E) in the Central Pyrenees (Camarero, unpub. data) as explained below.

Chloride concentration was assumed to be conservative, thus Cl^- concentration in precipitation was calculated from the concentration in the lake after correcting for 15% evapo-transpiration. Evapo-transpiration was estimated from the difference in Cl^- concentration (yearly volume weighted average) in precipitation and runoff from seven experimental catchments in the Central Pyrenees (Altuna, 2006).

Sodium was slightly enriched in precipitation with respect to Cl^- in the sea salt ratio by a factor of 1.15, as observed in previous studies (Camarero and Catalan, 1993), owing to terrigenous dust inputs. Potassium concentration was assumed to be low and constant throughout (5 $\mu eq\ l^{-1}$). Calcium deposition (Fig. 2a) depended on the location, with concentration decreasing from east to west (Camarero and Catalan, 1993). This Ca^{2+} gradient is caused by larger inputs of dust in the Eastern part of the Pyrenees, which has a stronger Mediterranean influence. Calcium concentration in precipitation for 2000 was extrapolated from measurements at Lake Redon in 2000, according to the observed gradient. Magnesium concentration was only 10% of that of Ca^{2+} in precipitation.

Sulphate (Fig. 2b) and inorganic N (Fig. 2c) were derived from EMEP model simulations (Tarrason, pers. comm.) after scaling with measurements at Lake Redon.

There are no available measurements of atmospheric deposition chemistry along the whole Pyrenean range that can be used to validate the gradients shown in Fig. 2. Therefore, these gradients can only be considered hypothetical. However, for the purpose of comparing two model runs these estimates provide, according to Lake Redon measurements, a reasonable, realistic input.

Estimates of base cation uptake by plants were the same as in Camarero et al. (2004). N dynamics were calibrated for each catchment and the major processes were nitrification, ranging between 80 and 100% of the annual NH_4^+ deposition, and NO_3^- uptake, ranging between 50 and 100% of the total NO_3^- supply (nitrification + deposition).

Weathering of S was adjusted for each catchment so as to account for the SO_4^{2-} excess in lake water, and was in the range 0–2000 meq m^{-2} yr^{-1}. In the Pyrenean catchments, sulphur comes from slates bearing pyrites and rocks with Ca and Mg sulphate minerals (Catalan et al., 1993).

Past EMEP scenarios for S (Mylona, 1993) and N (Alveteg et al., 1998) deposition and future B1 scenario for S and N (Amann et al., 1996) were used for hindcasting and forecasting (Fig. 3), as described in Camarero et al. (2004). The B1 scenario predicts the cost-minimal allocation of emission reductions to attain a decrease of the area of ecosystems with deposition above the critical load by at least 50% by 2010 in the European Union.

3. Results

The exact location of the soil profiles and their properties are shown in Table 3. The catchment-lumped soil parameters (measured) are shown in Table 4. Soils were poorly developed and thin, with an average depth of 37 (±std. dev=15) cm and

Table 4 – Soil lumped parameters for the catchments included in the study

	Depth	FEC	SC	pH_S	CEC	BS	TOC	C	N	C/N
	cm	kg m^{-3}	(%)		meq kg^{-1}	%	mol kg^{-1}	mol m^{-2}	mol m^{-2}	
Acherito	15.0	779	59	3.75	129.7	6.4	4.9	574	48	12.1
Bersau	19.7	896	59	4.10	47.5	14.2	2.3	399	33	11.9
Roumassot	23.3	734	72	4.28	52.6	24.3	5.0	779	54	14.1
Estom	9.9	361	31	4.21	85.7	29.2	8.5	323	21	15.6
Glacé	0.5	367	4	4.01	111.4	26.9	8.1	15	1	14.7
Gourg Cap de Long	0.2	385	1	4.76	74.6	83.5	4.1	3	0	13.7
La Munia Superior	5.3	643	8	4.62	30.8	61.6	1.5	38	4	10.4
La Munia Inferior	4.0	557	10	4.58	54.6	75.5	2.7	40	3	12.7
Port Bielh	16.5	552	38	4.04	73.0	13.3	4.7	501	33	15.2
Eriste	1.2	657	4	4.07	80.8	21.4	7.3	54	4	15.2
Redó	16.6	407	68	4.37	72.4	48.1	9.1	562	36	15.3
Pica Palomèra	21.0	883	70	3.88	36.5	14.1	4.3	794	33	23.8
Liat	16.1	564	70	3.89	80.6	17.3	4.8	435	26	16.9
Montoliu	15.4	641	50	4.04	57.9	19.7	3.8	331	24	14.8
Filià	27.3	617	52	4.29	44.5	36.1	1.8	311	28	11.0
Senó	14.2	929	42	4.25	43.4	9.1	5.1	664	47	14.4
Romedo Dalt	15.4	880	44	4.22	46.5	9.1	5.1	650	45	14.5
Colatx	20.0	929	40	4.26	38.0	8.5	4.9	913	66	13.9
Aixeus	4.1	594	18	4.00	70.8	30.6	7.2	175	11	15.4
Baiau	11.1	569	20	4.44	43.4	55.1	3.2	108	10	11.0
Negre	17.0	612	85	4.49	98.0	72.6	4.0	418	27	15.7
Estelat	54.7	635	78	4.30	42.2	18.6	3.5	1140	79	14.8

Please cite this article as: Camarero L, et al, A method for upscaling soil parameters for use in a dynamic modelling assessment of water quality in the Pyrenees, Sci Total Environ (2008), doi:10.1016/j.scitotenv.2008.10.035

Table 5 – Equations obtained by stepwise multiple regression used to model soil parameters as a function of diverse environmental parameters

	Multiple regression equation	AdjR^2	p-value
1	CEC = 0.6818 + 7.4587 OC + 4.8571 LP	0.5543	7×10^{-4}
2	OC = 23.164 − 0.0475 SC + 2.9712 PluB% − 3.5299 Carb% + 0.8873 cos(Aspect) − 10.179 PPT	0.4916	4×10^{-2}
3	BS = −26.4247 + 12.438 LP − 10.823 cos(Aspect)	0.6716	3×10^{-5}
4	pH_S = 3.9502 + 0.0089 BS	0.6598	5×10^{-6}
5	C/N = −473.3511 + 11.3672 latitude* + 1.6914 longitude* + 0.278 catchment area	0.4837	1×10^{-2}
6	FEC = 1128.887 − 35.9467 OC − 68.0361 LP	0.5625	4×10^{-4}
7	C_{pool} = 558.4789 + 6.537747 SC − 88.3658 LP	0.7728	8×10^{-7}
8	N_{pool} = 40.1576 + 0.415927 SC − 6.0926 LP	0.7247	5×10^{-6}
9	Soil depth = 0.0136 + 0.3365 SC	0.6309	6×10^{-6}

All units as in Tables 2 and 4, except * (latitude and longitude in decimal format).

(FEC) of 645 (±180) kg m^{-3}, equivalent to 240 (±117) kg m^{-2}. There were extensive areas without soil in the catchments, and (SC) averaged only 42% (±27%); when averaged for the whole catchment, soil depth and FEC were therefore considerably decreased to 15 (±12) cm and 103 (±83) kg m^{-2}, respectively. The average CEC was 64 (±26) meq kg^{-1}, equivalent to 13 (±4) eq m^{-2} (or 6 (±4) eq m^{-2} as whole-catchment average). Soil base saturation was 32% (±24%), and soils had an acidic character with pH_S averaging 4.22 (±0.26). Organic carbon averaged 4.8 (±2.1) mol kg^{-1}. All these values were in the typical ranges for alpine soils, comparable for instance to measurements in soils from the Tatra Mountains in Central Europe (Kopáček et al., 2004). Soil cation exchange capacity was on average slightly lower than in the Tatras, and also in Scottish soils, as reported by Helliwell et al. (1998). In contrast, BS was higher in the Pyrenees than in the Tatras and Scotland, which have been more affected by acidification. Lake water chemistry (Table 2) ranged from very low (or even negative) to relatively high Alk_G waters. The lowest Alk_G corresponded either to lakes with very dilute waters in crystalline, insoluble bedrocks or lakes on metamorphic bedrocks (schists and slates bearing pyrites) that supplied large amounts of mineral acidity from S weathering. Generally a lower amount of S was weathered from other lithologies in the region. Lakes with the highest Alk_G corresponded to catchments with an occurrence of limestone.

The equations resulting from the stepwise multiple regression analysis, where the environmental variables without

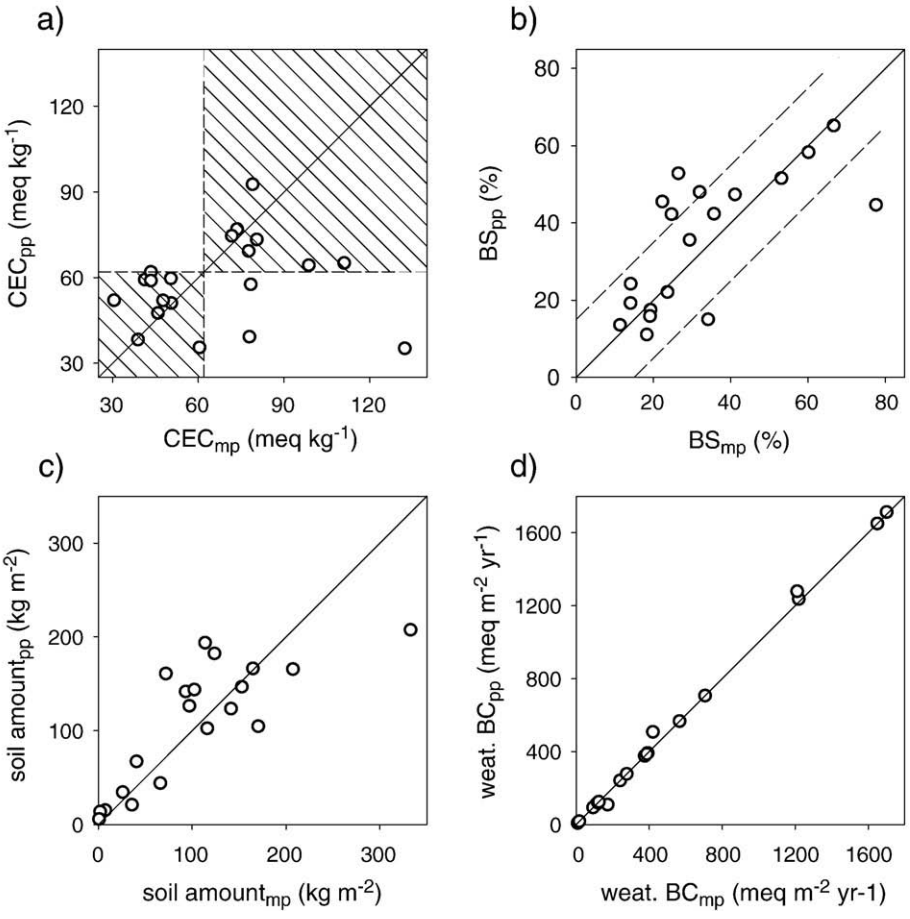

Fig. 4 – Comparison of measured and predicted input parameters used in the MAGIC simulations after calibration: a) CEC; b) BS; c) soil amount; d) base cation weathering. The subscript $_{mp}$ refers to measured values, $_{pp}$ indicates predicted values. The diagonal lines represent the 1:1 ratio. Shaded boxes in the CEC graph indicate the areas enclosing CEC values above and below 62 meq kg^{-1}. Dashed lines in the BS graph delimit the ±15% interval around the 1:1 line.

Please cite this article as: Camarero L, et al, A method for upscaling soil parameters for use in a dynamic modelling assessment of water quality in the Pyrenees, Sci Total Environ (2008), doi:10.1016/j.scitotenv.2008.10.035

explanatory value have been excluded, are shown in Table 5. The dependent variables in each equation are the soil input parameters required by MAGIC, and these equations were used to predict the values of the soil parameters to be compared against the actually measured parameters in the MAGIC runs. In most cases, we obtained highly significant ($p<10^{-4}$) multiple regressions explaining 55–77% of the amount of variance observed within the data set, as indicated by the adjusted regression coefficient (adjR^2). The correlation matrix for all environmental variables included in the equations was calculated to test for collinearity. All correlation coefficients were (in absolute value) less than 0.75, indicating that there was no collinearity. The weakest predictive power was for the C/N ratio ($p=0.01$, 48% of variance explained) and OC ($p=0.04$, 49% of variance). It should be noted that OC appeared in turn as a predictor for CEC and FEC, implying that, in practice, the predictability of the two latter variables is conditioned by the capacity to estimate the former. The same is true for BS and soil pH.

MAGIC was used to check the appropriateness of the predicted soil input parameters (i.e. those obtained with the multiple regression models) to simulate water chemistry. In the first calibration step, MAGIC computes a set of calibrated parameters for each lake by adjusting the input parameters provided initially as to obtain the best fit between observations and simulations for the target variables (i.e. the water chemistry). A comparison of the calibrated parameters CEC, BS, BC weathering and whole-catchment averaged soil amount obtained for each lake using their respective measured soil input parameters versus the calibrated parameters obtained using the predicted soil input parameters is shown in Fig. 4. CEC presented the worst correspondence between measured and predicted estimates. In practice, using Eqs. (1) and (2) (Table 5) CEC is effectively predicted above or below ~62 meq kg^{-1}. Soil base saturation (Eq. (3), Table 5) presented a better adjustment, with values falling in most cases within the ±15% interval around the 1:1 line. Soil amount was predicted using Eqs. (6) and (9) in Table 5, and the comparison with measured values showed a similar scatter to BS. The parameters CEC, BS and soil amount are relevant when calibrating the BC weathering rates in MAGIC. However, the deviation between observed and predicted BS, soil amount, and (to a larger extent) CEC had a minor effect on the weathering estimates, and generally a very good fit was obtained.

Hindcast and forecast simulations were used to assess the effect of the differences observed between measured and predicted input parameters on the performance of MAGIC. The MAGIC simulation of three key output variables (lake water SBC and ANC, and soil BS) obtained for each lake with measured and predicted soil input parameters are compared for the year 2040 (Fig. 5). Acid neutralising capacity (ANC) is computed by MAGIC as ANC = Σ base cations − Σ acid anions, and $Alk_G \approx$ ANC. Simulations of water chemistry were more consistent between the two methods than soil simulations. Predictions of BS maintained the same degree of uncertainty as the initial estimates for the calibration year (Fig. 4). The discrepancies were minor when comparing regional averages (Fig. 6). The simulated time series of SO_4^{2-} and ANC were virtually the same over the period 1850–2040, and SBC and BS presented parallel trajectories with differences of only ~3 μeq l^{-1} and ~2% respectively. According to the scenarios used here, both SO_4^{2-} and base cations in lake water increased since 1850, first at a slow rate and more rapidly from the 1940s onwards peaking in the 1980s and decreasing afterwards. By 2010, SO_4^{2-} will be at a level somewhat higher than in 1850. Instead, base cations concentration will reach the lowest levels in 2010 and increase slowly afterwards. The variation in base cations is lower than in

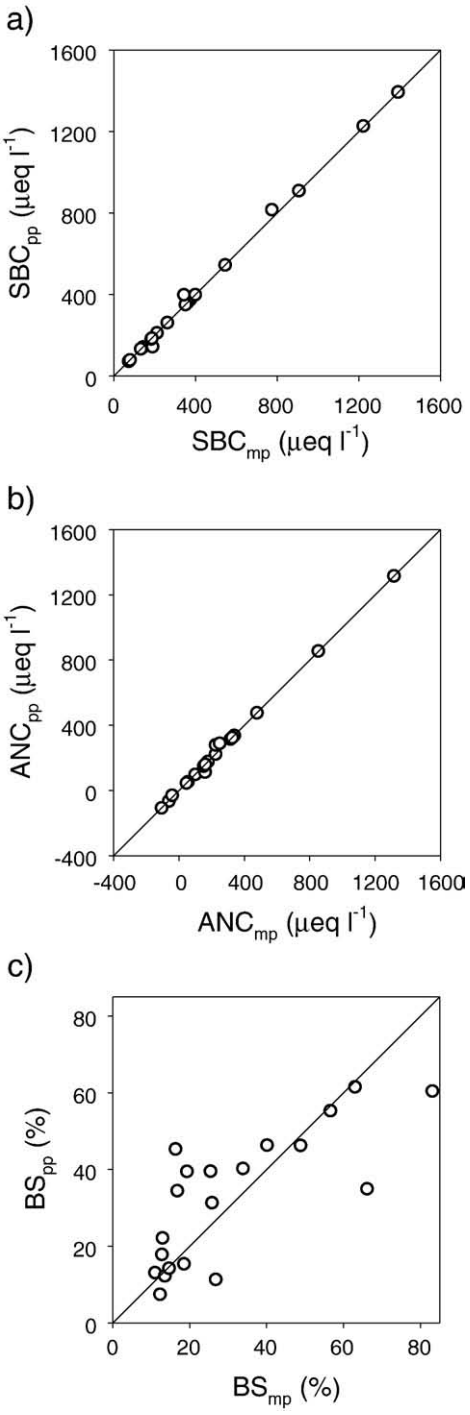

Fig. 5 – Comparison of the MAGIC projections of a) SBC, b) ANC and c) BS for 2040 obtained in each of the catchments studied by using measured input soil parameters (denoted by the subscript $_{mp}$) and predicted input soil parameters (denoted by the subscript $_{pp}$). The diagonal lines represent the1:1 ratio.

Please cite this article as: Camarero L, et al, A method for upscaling soil parameters for use in a dynamic modelling assessment of water quality in the Pyrenees, Sci Total Environ (2008), doi:10.1016/j.scitotenv.2008.10.035

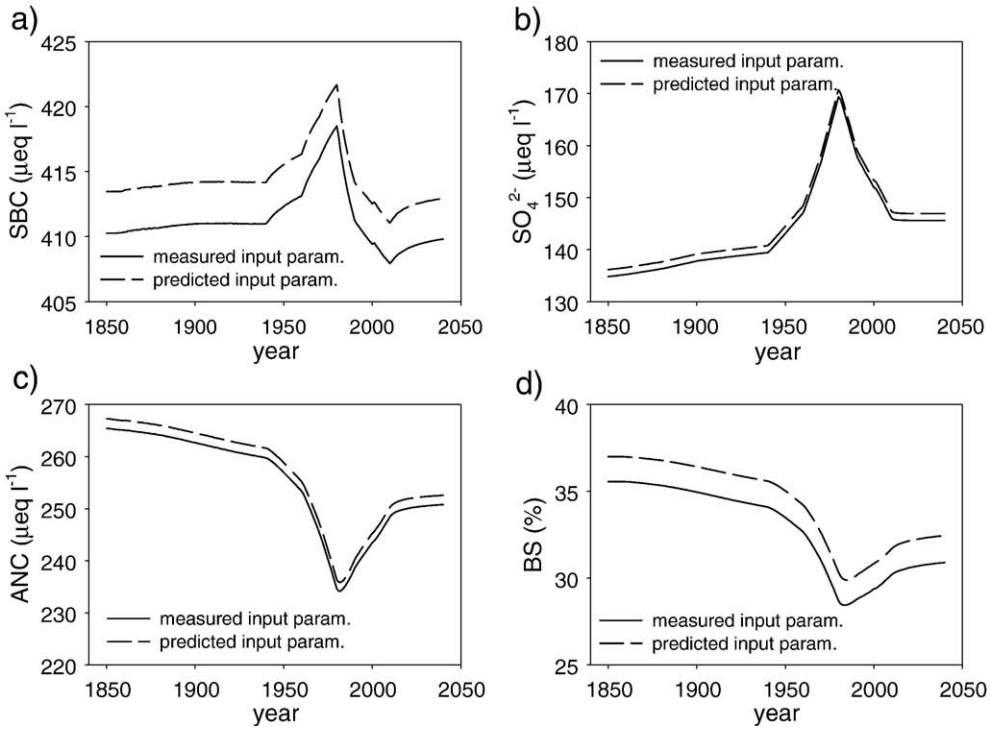

Fig. 6 – Time series of a) SBC, b) SO_4^{2-}, c) ANC and d) BS regional averages as simulated by MAGIC according to the deposition scenarios displayed in Fig. 3 for the period 1850–2040, using measured input soil parameters (solid line) and predicted input soil parameters (dashed line).

SO_4^{2-} in absolute terms. The result is a net loss of ANC between 1850 and 1980, more accentuated since 1940. After 1980, ANC would recover at a fast rate until 2010 and more slowly afterwards, but it would not reach the 1850 level by 2040. The BS trend is very similar to that of ANC.

4. Discussion

4.1. *Model performance using the predicted input values*

The good match between regional estimates using measured and predicted soil parameters indicated that the level of accuracy provided by the equations in Table 5 was sufficient to obtain acceptable regional results. As for individual catchment estimates, the simulation of water chemistry variables was better than for soil variables. While soil projections were largely determined by soil parameters, and were therefore sensitive to the uncertainty in the initial estimates, other additional parameters also contributed to determining water chemistry. Weathering rates are particularly relevant. Weathering rates were practically identical when computed using both measured and modelled soil input parameters, thereby indicating that the modelled values were of sufficient quality to allow adequate calibration. It is also likely that the relatively small amount of soil in high mountain catchments lowered the sensitivity of the calibration procedure to the soil properties compared with areas with greater soil presence, yielding thus robust estimates of weathering despite the relative uncertainty in modelling the soil parameters.

4.2. *Factors determining the soil properties*

Establishing the cause–effect relationships that underlie the empirical expressions listed in Table 5 was beyond the scope of this paper. Much more detail, based on individual samples rather than on lumped catchment parameters as done here, would be required to gain insight into these cause–effect relationships. This has been assessed elsewhere for OC storage in soils (Garcia-Pausas et al., 2007). Nevertheless, our results allowed us to propose a plausible hypothesis on the environmental factors that determine soil lumped properties.

Amongst all the multiple regression results, the most straightforward interpretation was for Eq. (9) (Table 5): given a typical soil depth of ~35 cm for mountain soils, the whole-catchment averaged depth was then directly proportional to the percentage of the catchment area covered by soil.

Eq. (4) also had a clear interpretation: there was a 'baseline' soil pH≈3.9, which increased proportionally to the saturation of bases that displaced exchangeable acidity from the soil exchange complex.

The best predictors for CEC (Eq. (1), Table 5) and FEC (Eq. (6)) were the same (OC and LP), but with opposite sign. As could be expected, OC was positively related to CEC because organic matter provides much of the cation exchange capacity in soils. The negative relation of OC with FEC may be associated with the reduction of bulk density as organic matter content is higher. The reason why LP showed similar behaviour was unclear, and we have not a satisfactory hypothesis for that.

In the case of BS (Eq. (3), Table 5), the effect of LP was as expected: more easily weathered rocks provided higher BS.

Please cite this article as: Camarero L, et al, A method for upscaling soil parameters for use in a dynamic modelling assessment of water quality in the Pyrenees, Sci Total Environ (2008), doi:10.1016/j.scitotenv.2008.10.035

The second parameter involved in BS was catchment aspect (cosine transformed), with south-facing catchments presenting higher BS than the north-facing ones. This relationship could reflect a degree of climatic control on either rock weathering or soil leaching. Greater insolation may cause higher temperatures and lower snow cover, which could result in greater frequency of freeze-thaw events and, consequently, increased weathering rates in south-facing catchments (Rech et al., 2001).

The C/N ratio (Eq. (5), Table 5) showed a correlation with both latitude and longitude, thereby suggesting geographic differences. Since this ratio was not related to any of the climatic parameters or proxies tested either here or in Garcia-Pausas et al. (2007), which could have suggested a geography–climate relationship, a biogeographic cause for this ratio can be argued. Plant species may make a significant contribution to determining C/N ratios in soils (Vinton and Burke, 1997). The distribution of species on the basis of the phytogeographic sectors defined along (longitude) and across (latitude) the main E–W axis of the Pyrenees (Vigo and Ninot, 1987; Ninot et al., 2007) could account for the geographic differences in C/N. Another possibility could be that geographic differences in N deposition would influence C/N in soils. However, our data do not seem to point to this. Fig. 2c shows that N deposition tends to be higher in the Central Pyrenees than in the other parts. In the Western Pyrenees N deposition is higher in the southern than in the northern slope, whereas in the Eastern Pyrenees the tendency is the opposite. Assuming that more N deposition would cause lower soil C/N, Eq. (5) would imply higher N deposition at lower latitude (southern face) and longitude (west), which does not clearly match the N deposition pattern described above.

C_{pool} and N_{pool} were closely related, and the same environmental variables (SC and LP) appeared as predictors of both parameters (Eqs. (7) and (8), in Table 5). Using the same rationale as for soil depth, their relationship with SC can be explained as the result of the whole-catchment averaging used to compute C and N pools. As LP had no relation with the organic matter content in any of the equations, it is reasonable to assume that the negative relation found here was, as already discussed for FEC, indicative of a smaller amount of soil and hence reduced soil pools.

OC was the parameter with the largest number of predictors involved and the most complex expression (Eq. (2)). It was also the parameter with the lowest significance in its estimation ($adjR^2=0.492$, $p=0.04$). The predictability of OC in soils can be improved by dealing with individual soil profiles and using a set of additional climatic and topographic variables ($adjR^2=0.569$, $p<0.001$, Garcia-Pausas et al., 2007). Nevertheless, the predictability of catchment-lumped parameters, as used here, did not show better performance when introducing these additional variables in the multiple regression fittings. This observation can be interpreted as an indication that the within-catchment variability was higher for OC than for the other parameters considered, possibly due to the influence of multiple factors, and that this small-scale heterogeneity hinders the estimation of lumped OC values. However, it is of interest to notice that Eq. (2) (Table 5) captures some of the main factors that act on OC (Garcia-Pausas et al., 2007). Thus, in both studies it was shown that plutonic rocks tend to favour higher OC values than other rock classes. One possible explanation is that base-poor plutonic rocks originate acid soils where decomposition rates are slower and OC accumulation is hence favoured. Nonetheless, this interpretation is not straightforward. The class of rocks appearing in Eq. (2) is PluB (Table 1), which are relatively soluble, and there are other kinds of rocks not included in the equation that could be expected to originate more acid soils. Instead, the same explanation relating soil acidity and OC seems to be more robust to explain why carbonated rocks appear with negative sign in Eq. (2).

Precipitation was negatively correlated with OC in our study, whereas Garcia-Pausas et al. (2007) found that, more specifically, summer PPT was negatively related to OC but only at the warmest sites. Aspect was a relevant predictor of OC in Garcia-Pausas et al. (2007) work, but there was a complex response involving a direct effect of aspect and its interactions with summer PPT and water stress, with the result that at the highest altitudes OC was greater on southern aspects, whereas at the lowest altitudes OC was increased on northern aspects. In the present study, aspect also appeared as a factor determining OC, but the dominant effect was that northern aspects favoured higher OC than southern aspects. When considering whole catchments, the lower water deficit in north-facing catchments appeared to counterbalance the less favourable temperature conditions for plant growth, thus favouring soil OC accumulation.

4.3. *History of soil acidification*

The trends shown in Fig. 6 describe the effects of atmospheric acid deposition, which had its maximum spread in the 1960s–80s, in the Pyrenean catchments. Most Pyrenean lakes lie in catchments with granitic bedrocks and are thus sensitive to acid deposition. Despite this sensitivity, acidification has had little effect, partly because the atmospheric acid load has been moderate compared with Central and Northern Europe, and partly because of the neutralising effects of the natural inputs of airborne base cations from the Iberian Peninsula and Northern Africa. On the basis of the assumptions described above, i.e. taking into account EMEP reconstructions of S and N deposition over Europe, the B1 future scenario, and omitting possible changes in airborne base cations and weathering rates, our simulations indicate that the main acidifying effect was caused by an increase in SO_4^{2-} in lake water, which was partly compensated by a rise in base cations displaced from the soil exchange complex. On average, this process caused a regional ANC loss of ~30 μeq l^{-1} compared to pre-industrial levels. This figure is consistent with a previous estimate (35 μeq l^{-1}, Camarero and Catalan, 1998), which was obtained with a different model and data set. Acidification of Pyrenean soils has also caused an average decrease in BS of ~7%. According to the model, both ANC and BS have started to recover since the 1980s. By 2008, ANC has increased in ~13 μeq l^{-1} and BS in ~1.5%. However, although B1 provides an 'optimistic' scenario, projections of future atmospheric deposition using this scenario indicate that pre-industrial levels will not be attained by 2040. To achieve this, EU member countries should reduce their S and N emissions further than what is established in the reduction plan agreed and in current legislation.

Please cite this article as: Camarero L, et al, A method for upscaling soil parameters for use in a dynamic modelling assessment of water quality in the Pyrenees, Sci Total Environ (2008), doi:10.1016/j.scitotenv.2008.10.035

5. Conclusions

The main aim of this study was to derive soil parameters for regional scale model applications. The empirical relationships established here allowed us to model and predict these parameters as a function of a set of environmental variables used as predictors.

When used as an input for the biogeochemical dynamic model MAGIC, the predicted soil parameters allowed acceptable simulations of the water chemistry and soil base saturation in Pyrenean mountain catchments. There was some uncertainty in estimating soil properties from the proposed regression models. When catchments were examined individually, this uncertainty was transmitted to the simulation results for soils, but had a minor effect on water chemistry simulations. When assessing regional averages, the error associated with the initial estimates did not cause a significant deviation of simulations based on predicted soil input parameters from those based on field measures, either for water or soil chemistry.

Several soil parameters were predicted by simple models with a relatively straightforward physico-chemical interpretation. Thus, for instance, soil pH was related to BS, and BS was in turn associated with the proportion of easily weathered rocks. The parameters that were expressed as whole-catchment averages (such as soil depth, C_{pool}, and N_{pool}) were strongly dependent on the percentage of soil coverage in the catchment (SC). The C/N ratio showed a geographic dependence.

The most difficult predictions, i.e. involving the largest number of predictors, the most complex expression, and the lower level of significance, were for OC, which appears in turn in the equations as a predictor of other key soil properties, like CEC and FEC. The small-scale heterogeneity associated with the relationships between plants and soil biology, climate, and topography probably account for such complexity in the prediction.

The methodology described here proved to be a useful approach to upscale soil properties in the Pyrenean area, and is potentially applicable to other regions that lack extensive soil information. Using the method proposed, the soil data required for dynamic hydrochemical modelling can be inferred with sufficient accuracy from available mapped (topography, lithology and climate) and remotely sensed (landcover) information.

Acknowledgments

M. Ventura and J. Catalan (CSIC) provided the GIS data. L. Tarrason and A. Benedictow (EMEP) supplied the atmospheric deposition model estimates. R. Thompson (Univ. Edinburgh) provided temperature and precipitation estimates. B.J. Cosby and R.F. Wright provided the MAGIC model. This study was funded partly by the European Union (EMERGE project EVK1-CT-1999-00032 and Eurolimpacs project GOCE-CT-2003-505540) and the Spanish Ministry of Science and Technology (CICYT grant REN2000-0889/GLO). This study is a result of the activities of the Limnological Observatory of the Pyrenees (LOOP), a joint initiative of the Centre for Advanced Studies of Blanes-CSIC and the Centre for High Mountain Research — University of Barcelona.

REFERENCES

Agustí-Panareda A, Thompson R. Reconstructing air temperature at eleven remote alpine and arctic lakes in Europe from 1781 to 1997 AD. J Paleolimnol 2002;28:7–23.

Altuna M. Estudio de la dinámica hidro-biogeoquímica y balances de masa elementales en cuencas de alta montaña: una aproximación a algunos aspectos del ciclo del carbono. M. Sc. Thesis, Universitat de Girona, 2006, 113 pp.

Alveteg M, Walse CC, Warfvinge P. A method for reconstructing historic deposition and uptake from present day values using MAKEDEP. Water Air Soil Pollut 1998;104:269–83.

Amann M, Bertok I, Cofala J, Gyarfas F, Heyes C, Klimont Z, et al. Cost-effective control of acidification and ground-level ozone. Second Interim Report to the European Commission, DG XI. IIASA; 1996. December, 112 pp.

Camarero L, Catalan J. Chemistry of bulk precipitation in the Central and Eastern Pyrenees (Northeast Spain). Atmos Environ 1993;27A:83–94.

Camarero L, Catalan J. Variability in the chemistry of precipitation in the Pyrenees (northeastern Spain): dominance of storm origin and lack of altitude influence. J Geophys Res 1996;101:29491–8.

Camarero L, Catalan J. A simple model of regional acidification for high mountain lakes: application to the Pyrenean lakes (North-East Spain). Water Res 1998;32:1126–36.

Camarero L, Wright RF, Catalan J, Ventura M. Application of MAGIC to Lake Redó (Central Pyrenees): an assessment of the effects of possible climate driven changes in atmospheric precipitation, base cation deposition, and weathering rates on lake water chemistry. J Limnol 2004;63:123–32.

Camarero L, Rogora M, Mosello R, Anderson J, Barbieri A, Botev I, et al. Regionalisation of chemical variability in European mountain lakes. Freshwater Biol, in press.

Casals-Carrasco P, Catalan J, Madhavan B, Gond V. A spectral approach to model mountain lake catchment through landscape attributes. Proc. SPIE Int. Soc. Opt. Eng. 2004;5239:145–64.

Catalan J, Ballesteros E, Gacia E, Palau A, Camarero L. Chemical composition of disturbed and undisturbed high mountain lakes in the Pyrenees: a reference for acidified sites. Water Res 1993;27:133–41.

Cosby BJ, Hornberger GM, Galloway JN, Wright RF. Modelling the effects of acid deposition: assessment of a lumped parameter model of soil water and streamwater chemistry. Water Resour Res 1985a;21:51–63.

Cosby BJ, Wright RF, Hornberger GM, Galloway JN. Modelling the effects of acid deposition: estimation of long term water quality responses in a small forested catchment. Water Resour Res 1985b;21:1591–601.

Cosby BJ, Ferrier RC, Jenkins A, Wright RF. Modelling the effects of acid deposition: refinements, adjustments and inclusion of nitrogen dynamics in the MAGIC model. Hydrol Earth Syst Sci 2001;5:499–518.

Garcia-Pausas J, Casals P, Camarero L, Huguet C, Sebastià MT, Thompson R, et al. Soil organic carbon storage in mountain grasslands of the Pyrenees: effects of climate and topography. Biogeochemistry 2007;82:279–89.

Harvey LDD. Upscaling in global change research. Clim Change 2000;44:225–63.

Helliwell RC, Ferrier RC, Evans CD, Jenkins A. A comparison of methods for estimating soil characteristics in regional acidification models; an application of MAGIC model to Scotland. Hydrol Earth Syst Sci 1998;2:509–20.

Hettelingh J-P, Posch M, Slootweg J. Status of European critical loads and dynamic modelling. In: Posch M, Hettelingh J-P, Slootweg J, Downing RJ, editors. Modelling and Mapping Of

Please cite this article as: Camarero L, et al, A method for upscaling soil parameters for use in a dynamic modelling assessment of water quality in the Pyrenees, Sci Total Environ (2008), doi:10.1016/j.scitotenv.2008.10.035

Critical Thresholds In Europe, CCE Status Report, 2003. RIVM Report 259101013. Bilthoven: RIVM; 2003. p. 1–10.
Kopáček J, Stuchlík E, Veselý J, Schaumburg J, Anderson IC, Fott J, et al. Hysteresis in reversal of central European mountain lakes from atmospheric acidification. Water Air Soil Pollut Focus 2002;2:91–114.
Kopáček J, Kaňa J, Šantrůčková H, Picek T, Stuchlík E. Chemical and biochemical characteristics of alpine soils in the Tatra Mountains and their impact on lake water quality. Water Air Soil Pollut 2004;153:307–27.
Mylona S. Trends of sulphur dioxide emissions, air concentrations and depositions of sulphur in Europe since 1880. EMEP/MSC-W Report 2/93. Oslo: The Norwegian Meteorological Institute; 1993. 99 pp.
Ninot JM, Carrillo E, Font X, Carreras J, Ferré A, Masalles RM, et al. Altitude zonation in the Pyrenees. A geobotanic interpretation. Phytocoenologia 2007;37:371–98.
Olendrzynski K, Jonson JE, Bartnicki J, Jakobsen HA, Berge E. EMEP Eulerian model for acid deposition over. Europe Int J Environ Pollut 2000;14:391–9.
Prechtel A, Alewell C, Armbruster M, Bittersohl J, Cullen JM, Evans CD, et al. Response of sulphur dynamics in European catchments to decreasing sulphate deposition. Hydrol Earth Syst Sci 2001;5:311–25.
Rech JA, Reeves RW, Hendricks DM. The influence of slope aspect on soil weathering processes in the Springerville volcanic field, Arizona. Catena 2001;43:49–62.
Rodhe H, Grennfelt P, Wisniewski J, Ågren C, Bengtsson G, Johansson K, et al. Acid Reign '95 — Conference Summary Statement. Water Air Soil Pollut 1995;85:1–14.
Stoddard JL, Jeffries DS, Lükewille A, Clair TA, Dillon PJ, Driscoll CT, et al. Regional trends in aquatic recovery from acidification in North America and Europe 1980–95. Nature 1999;401:575–8.
Thomas GW. Exchangeable cations. In: Page AL, Miller RH, Keeney DR, editors. Methods of Soil Analysis, Part 2. Agron. Soc. Amer. and Soil Sci. Soc. Amer., 2nd ed.Madison; 1982. p. 159–66.
Vigo J, Ninot JM. Los Pirineos. In: Peinado-Lorca M, Rivas-Martínez S, editors. La vegetación de España. Madrid: Servicio Publicaciones Universidad Alcalá de Henares; 1987. p. 351–84.
Vinton MA, Burke IC. Contingent effects of plant species on soils along a regional moisture gradient in the Great Plains. Oecologia 1997;110:393–402.
Wright RF, Larssen T, Camarero L, Cosby BJ, Ferrier RC, Helliwell R, et al. Recovery of acidified European waters. Environ Sci Technol 2005;39(3):64A–72A.
Wright RF, Aherne J, Bishop K, Camarero L, Cosby BJ, Erlandsson M, et al. Modelling the effect of climate change on recovery of acidified freshwaters: relative sensitivity of individual processes in the MAGIC model. Sci Total Environ 2006;356:154–66.

Please cite this article as: Camarero L, et al, A method for upscaling soil parameters for use in a dynamic modelling assessment of water quality in the Pyrenees, Sci Total Environ (2008), doi:10.1016/j.scitotenv.2008.10.035